Multisensor analysis of integrated atmospheric water vapor over Canada and Alaska

A. I. Bokoye,[1,2] A. Royer,[1] N. T. O'Neill,[1] P. Cliche,[1] L. J. B. McArthur,[3] P. M. Teillet,[4] G. Fedosejevs,[4] and J.-M. Thériault[5]

Received 3 July 2002; revised 22 March 2003; accepted 2 April 2003; published 14 August 2003.

[1] Atmospheric water vapor is a key parameter for the analysis of climatic systems (greenhouse gas effect), in particular over high latitudes where water vapor displays an important seasonal variability. The sparse spatial and temporal sampling of atmospheric water vapor observations across Canada needs to be improved. A series of instruments and methods including a 940-nm solar absorption band radiometer (R) and radiosonde (S) analysis from a numerical weather prediction model and a ground-based bi-frequency Global Positioning System (GPS) were used to evaluate the integrated atmospheric water vapor (IWV) at various sites in Canada and Alaska from a multiyear database. The IWV-R measurements were collected within the framework of the North American Sun Radiometry network (AERONET/AEROCAN). Intercomparisons between [IWV-GPS and IWV-S], [IWV-R and IWV-GPS], and [IWV-R and IWV-S] show root mean square (RMS) differences of 1.8, 1.9, and 2.2 kg m^{-2}, respectively. GPS meteorology appears to be the easiest approach to calibrate the solar radiometer water vapor band owing to its flexibility, and it allows us to overcome the Sun radiometry limitation in high-latitude areas like the Arctic. The sensitivity of the GPS retrieval to various parameters like GPS satellite constellation and meteorological data are discussed. The classical linear relationship between the surface temperature and the integrated weighted mean temperature profile needed for IWV-GPS retrieval may be significantly different for Arctic air masses compared with midlatitude air masses in the case of tropospheric temperature profile inversion. An ever-expanding multiyear (1994–2001) North American summer water vapor climatology, derived from AERONET/Canadian Sun Radiometer Network, is presented and analyzed, showing a mean value of 19.8 ± 6.1 kg m^{-2} and variations from 17 kg m^{-2} in Alaska to 23 kg m^{-2} in southeastern Canada. The results in Bonanza Creek, Alaska, show significant interannual variations with a peak in 1997, which may be linked to an El Niño event that occurred in the same year. Such a database may also be useful for climate model validation as shown for the Canadian Global Environmental Model (RMS difference of 3.4 kg m^{-2}). In the end we show that, even if data are selected only for cloud-free atmospheres, there are no significant differences as compared with radiosonde climatology at Canadian Northwestern sites ($\leq$3% relatively to Bonanza Creek summer mean value). *INDEX TERMS:* 0365 Atmospheric Composition and Structure: Troposphere—composition and chemistry; 0394 Atmospheric Composition and Structure: Instruments and techniques; 0933 Exploration Geophysics: Remote sensing; 1655 Global Change: Water cycles (1836); *KEYWORDS:* atmosphere, integrated water vapor, GPS, solar radiometer, radiosonde, model

Citation: Bokoye, A. I., A. Royer, N. T. O'Neill, P. Cliche, L. J. B. McArthur, P. M. Teillet, G. Fedosejevs, and J.-M. Thériault, Multisensor analysis of integrated atmospheric water vapor over Canada and Alaska, *J. Geophys. Res.*, *108*(D15), 4480, doi:10.1029/2002JD002721, 2003.

[1]Centre d'Applications et de Recherches en Telédétection, Université de Sherbrooke, Sherbrooke, Quebec, Canada.

[2]Now at Laboratoire Interdisciplinaire en Sciences de l'Environnement/Ecosystèmes Littoraux et Côtiers, Université du Littoral Côte d'Opale: Maison de la Recherche en Environnement Naturel, Wimereux, France.

[3]Meteorological Service of Canada, Downsview, Ontario, Canada.

[4]Canada Centre for Remote Sensing, Ottawa, Ontario, Canada.

[5]Defence Research and Development Canada, Valcartier, Valcartier, Quebec, Canada.

0148-0227/03/2002JD002721$09.00

1. Introduction

[2] The recent analysis of global and regional climatic system trends is characterized by nonlinear changes and some extreme events in the context of global climate changes. The evaluation of the magnitude and the impact of water vapor feedback [*Held and Soden*, 2000] are the major uncertainties for a comprehensive understanding of the global climate system. Until now, poor knowledge of the global distribution of tropospheric water vapor (the most important greenhouse gas) in space and time has limited the

accurate prediction of weather and climate using numerical models. Furthermore, atmospheric water vapor plays an important role in climatic processes such as the global hydrologic cycle through precipitation [*Hall and Manabe*, 2000] and evapotranspiration and the radiative energy balance and its impact on clouds and aerosols [*Kay and Box*, 2000]. Water vapor content feedback also appears to be a key element in Arctic climate that influences the global climate system [*Blanchet and Girard*, 1994, 1995; *Curry et al.*, 1995; *Bokoye et al.*, 2002].

[3] Over the past decades, numerous space- and ground-based techniques, as well as numerical simulations, were developed to improve the monitoring of atmospheric water vapor. The present study focused on ground-based techniques and investigated the following methods.

[4] 1. Ground-based solar radiometers operating in the strong water vapor absorption band at 940 nm allowing the retrieval of total atmospheric water column abundance when the path to the Sun is free of clouds [*Schmid et al.*, 1996, 2001; *Halthore et al.*, 1997].

[5] 2. Operational meteorological soundings and numerical model simulations to estimate water vapor content. The Meteorological Service of Canada (MSC), like other national weather services in the world, uses balloon-borne radiosondes deployed at 0000 and 1200 UT to measure the total atmospheric water vapor content [*Elliot and Gaffen*, 1991]. The radiosondes can provide data up to the 50-hPa atmospheric pressure level or higher representing at least 90% of the water vapor in a vertical atmospheric column. This technique remains the reference method used for weather forecasts despite the associated problems of increasing operational costs, infrequent launches, and the limited number of observation locations to adequately characterize water vapor spatial variability. These meteorological observations are assimilated by numerical weather prediction models (NWPM) like that of *Côté et al.* [1997] as initial conditions required for accurate prediction.

[6] 3. Global Positioning System (GPS) constellation satellites (up to 28 operational satellites positioned 20,000 km above the surface of the Earth) can be used to monitor water vapor amounts within ±1 to ±2 kg m^{-2} accuracy. Numerous recent studies confirm the feasibility of estimating the integrated atmospheric water vapor (IWV) from GPS meteorology across the world [*Niell et al.*, 2001; *Ohtani and Naito*, 2000; *Liou et al.*, 2000; *Sierk et al.*, 1997] since its basic concept was established by *Bevis et al.* [1992, 1994]. The main advantages of GPS water vapor meteorology are the high temporal resolution of IWV retrievals, the capability of operating under all weather conditions, the absence of calibration constraints, and its relatively low cost compared to other methods. Thus GPS meteorology appears to be the most appropriate technique for accurate climate and weather predictions in the future by data assimilation [*Baker et al.*, 2001].

[7] Note that other ground-based water vapor techniques that are not considered in this paper can be very useful for the assessment of atmospheric water vapor content from ground-based measurements. One can mention the Raman lidar and differential absorption lidar techniques used to retrieve water vapor profiles in the troposphere [*England et al.*, 1992; *De Tomasi et al.*, 2000]. The infrared Sun radiometric method based on the atmospheric hygrometry technique is also used for the retrieval of water vapor amounts from an absorption model in the atmosphere [*Tomasi et al.*, 2000; *Sierk et al.*, 1997]. Microwave radiometry can also be used to estimate atmospheric water vapor content from a dual-frequency system operating at 20.6 and 31.65 GHz. These frequencies are very sensitive to the column integrated water vapor and liquid water present in the lower part of the troposphere [*Hogg et al.*, 1983; *Westwater*, 1978; *Westwater et al.*, 1990]. The Atmospheric Emitted Radiance Interferometer (AERI) can be used to create water vapor profiles in the Planetary Boundary Layer (PBL) or the lower 3 km of the Earth's atmosphere. AERI passively measures infrared (IR) radiation (3–18 μm), yielding high wave number resolution radiance spectra (<1 cm^{-1}). These radiance spectra are transformed into vertical temperature and water vapor profiles by inverting the IR radiative transfer equation [*Thériault et al.*, 1996; *Feltz et al.*, 1998; *Smith et al.*, 1998].

[8] The present work was carried out in the framework of the Canadian Sun Radiometer Network (AEROCAN) deployment (Figure 1). AEROCAN is a member of the worldwide federated network Aerosol Robotic Network (AERONET) (available at http://aeronet.gsfc.nasa.gov) based at the NASA Goddard Space Flight Center (GSFC). A complete description of the AEROCAN network can be found in *Bokoye et al.* [2001]. In addition to atmospheric aerosol characterization, this network can provide a continuous multiyear Canadian water vapor climatology.

[9] The aim of this paper is to present some characteristics of water vapor time series derived from AERONET/AEROCAN's solar radiometer IWV estimates in the Canadian and Alaskan weather context and to assess this approach as compared to radiosonde and GPS meteorology. Specific consideration will be given to high-latitude water vapor analysis.

[10] The data from the four different sources will be described in section 2. The results of the intercomparisons and GPS meteorology characteristics in Canada are analyzed and discussed in section 3. Water vapor climatology is presented in section 4 with an application for climate model validation. The main conclusions will be highlighted with the perspective of developing an improved atmospheric water vapor monitoring system.

2. Data Acquisition and Processing

2.1. Canadian Water Vapor Radiometer Network: AEROCAN

[11] The Canadian Sun Radiometer network is equipped with Cimel™ Sun radiometers [*Holben et al.*, 1998]. These instruments permit the retrieval of IWV from direct solar measurement in the strong water absorption band at 940 nm assuming a fixed calibration constant [*Halthore et al.*, 1997]. The measurements are taken every 15 min between solar air masses of 1.7 and 7. Note that the air mass is the ratio of the atmospheric path length through which direct solar radiation beam will pass to the path length it would pass through if the sun were at the zenith.

[12] A Cimel data logger directs the acquired data to a data collection platform that controls hourly data transmission to Geostationary Operational Environmental Satellite (GOES). The data are then relayed to a ground receiving

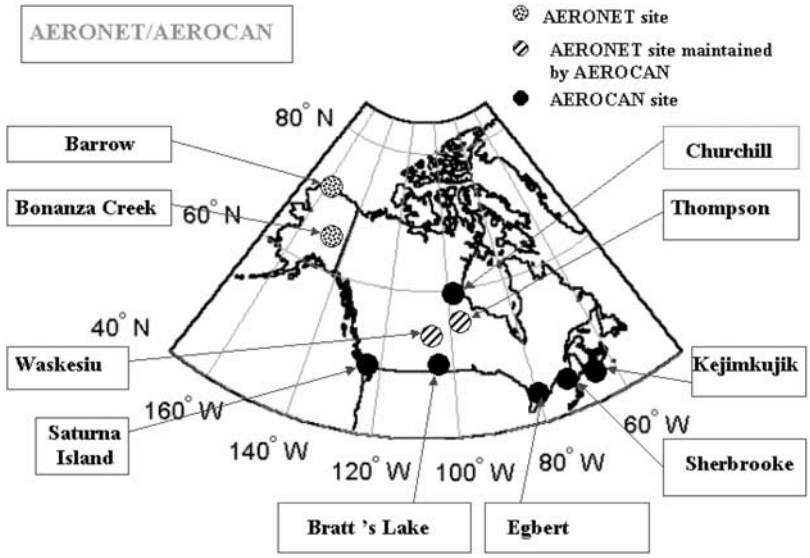

Figure 1. Canadian Sun Radiometer Network/Aerosol Robotic Network (AEROCAN/AERONET) site location map.

station. They are then processed and archived according to a standardized procedure for the AERONET network [*Holben et al.*, 1998] at GSFC. The AEROCAN and AERONET staff ensure the quality of data collected on a weekly basis. An accurate retrieval of IWV from solar transmittance methods [*Schmid et al.*, 2001] necessitates accurate calibration of the network instruments.

[13] Figure 1 displays the AEROCAN water vapor radiometer (Sun radiometer) network across Canada and Alaska. The water vapor data used for this study cover the period from 1994 to 2001. These data were recorded simultaneously with aerosol optical depth. AEROCAN/AERONET network level 1.5 data (cloud screened) with an additional screening step that is tied to the value of the Angström exponent [*Bokoye et al.*, 2001] are considered. In order to eliminate erroneous IWV values, a constraint of IWV variation limit between 0 and 4 kg m^{-2} appropriate for the latitudes considered was also retained.

2.2. GPS Observations and Methodology

[14] Two GPS field measurement campaigns were carried out at Sherbrooke (45°22′N, 71°55′W) and Valcartier (46°54′N, 71°30′W) with a temporal resolution of 30 s. The principle of these measurements is based on the constellation of GPS satellites that continuously transmit on two carrier frequencies, 1575.42 and 1227.60 MHz, referred to as L1 and L2, respectively.

[15] The ionosphere, the troposphere, and instrumentation errors introduce propagation delay into the path length of these signals. The IWV can be estimated from the separation of the neutral atmospheric delay (~2 m at zenith) from the other delays like ionospheric, geometric, and clock delays. The GPS community has developed a methodology [*Bevis et al.*, 1992, 1994] to compute the neutral atmosphere (mainly the tropospheric) delay. The latter is a product of the neutral mapping function [*Niell*, 1996] and the zenithal tropospheric delay (ZTD). The neutral delay includes the hydrostatic or dry delay (ZHD) and the delay caused by water vapor (ZWD), which is proportional to the amount of water vapor. Above 15° of elevation the wet and dry mapping functions differ only very slightly [*Duan et al.*, 1996]; thus ZTD is simply the sum of the dry and wet components in the zenith direction. The coefficient of proportionality between IWV and ZWD is a linear function of the weighted mean atmospheric temperature [*Davis et al.*, 1985]. Appendix A gives a summary of this method as reported by numerous authors [*Bevis et al.*, 1992, 1994, 1996; *Duan et al.*, 1996; *Liou et al.*, 2000; *Iwabuchi et al.*, 2000].

[16] Atmospheric water vapor, mainly concentrated in the first 5 km, introduces a propagation delay in these signals between GPS satellites and the receiver. The GPS meteorology varies according to the geometry of the satellite constellation, essentially satellite elevation and water vapor scale height (Figure 2). For this study the GPS receiver used was a Novatel, Inc. Millenium OEM3 unit associated with a PowerPak II hardware interface. This unit allows tracking of the L1 and L2 carrier phase of up to 12 satellites. The antenna used with this receiver is a new Novatel, Inc. GPS-600 antenna. The latter is an active antenna designed to operate at the GPS L1 and L2 frequencies. This antenna employs Novatel's Pinwheel aperture coupled slot array technology instead of the conventional patch design methods. Its radiation pattern is shaped to reduce signals arriving at low elevation angles; these features decrease the errors associated with electromagnetic interference and multipath effects [*Kunysz*, 2000]. VIASAT, Inc. (Montreal, Quebec, Canada) acquisition software EZ-Surv is used to acquire observation and navigation files in standard daily Receiver Independent Exchange (RINEX) format. RINEX file data containing satellite to receiver range/distance (code) and phase measurements (carrier) data are postprocessed using the Geodetic Survey Division GPSpace software (Geodetic Survey Division, Natural Resources Canada, Ottawa, Ontario, Canada). The latter applies precise satellite clock corrections and orbital information (ephemerides) that are computed from the International GPS Service (IGS) networks to improve positioning accuracy. Note that GPS data

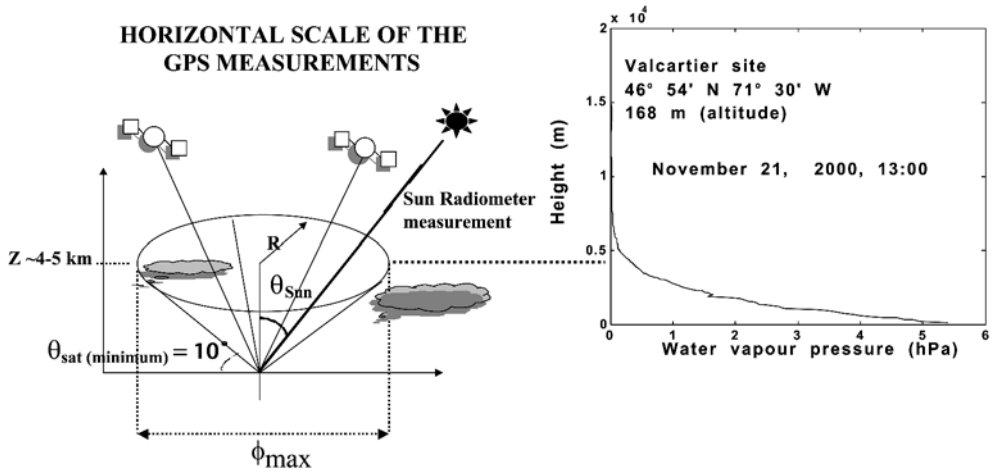

Figure 2. Principle of water vapor retrieval from Global Positioning System (GPS) meteorology. The spatial representativeness of GPS-derived Integrated Water Vapor (IWV-GPS) for a given observation site can be as large as an area with a 50-km diameter (ϕ_{max}). (right) The example of altitude as function of water vapor pressure shows that the major part is concentrated in the lower 5 km of the troposphere.

in RINEX format, processed sequentially in time and independent positions, can reach accuracies (RMS error) of a few centimeters or less using code and phase observations for every period where four or more satellites are available. In addition to the processing system the achievable accuracy depends on the performance of the user's receiver (measurement noise) and errors introduced by the multipath present at the observation site. In the context of this study this accuracy is computed from comparison between GPSpace-derived positions and International Terrestrial Reference Frame 2000 (ITRF2000) reference sites.

[17] GPSpace applies the precise point-positioning technique (also called absolute point positioning or single point positioning) for each daily RINEX file [*Héroux et al.*, 1993; *Zumberge et al.*, 1997; *Kouba and Héroux*, 2001]. This method applies separate corrections for some of the errors as opposed to applying a combined correction in the case of relative positioning using a local differential approach based on a GPS network [*Hurn*, 1993]. This method depends on precise satellite clock corrections and a precise ephemeris to correct for GPS-satellite-based errors in the user-observed ranges. These data are available by ftp for the GPS community from the IGS Central Bureau at the NASA Jet Propulsion Laboratory (JPL) (available at http://igscb.jpl.nasa.gov/components/prods_cb.html). Since these products are based on a network of known accurate reference locations equipped with high-quality geodetic-type receivers, uncertainties associated with using corrections from a single base station are effectively removed. Dual-frequency users have the advantage of two frequencies to remove the delay introduced by the ionosphere using a linear combination from L1 and L2 [*Dong and Bock*, 1989]. In fact, ionospheric refractivity depends on the frequency. The magnitude of this delay, which depends on the latitude, season, time of day and level of solar activity, can reach a maximum value of 20 m at sunspot maximum in North America. However, it should be noted that the impact of ionospheric delay on positioning accuracy is generally concentrated in the vertical component of the position. For single-frequency users, considerable effort has been made to establish models that minimize this effect [*Rocken et al.*, 2000]. The remaining positioning accuracy limitations are site-dependent and cannot be improved using differential corrections. These limitations include the user's receiver code resolution (measurement noise) and the multipath effect present at the observing site [*Lachapelle et al.*, 1990; *Georgiadou and Kleusberg*, 1988; *Van Dierendonck et al.*, 1992]. Our GPS antenna is located such that it is free of any obstacles on the horizon in order to reduce multipath errors. Furthermore, GPSpace applies a correction to GPS-600 antennae phase center variations to remove induced receiver-satellite range errors, which can be significant for satellite elevations <10°. A cutoff angle (mask angle) of 10° has been retained for GPS records, supposedly independent of azimuthal effects (Figure 2). The ITRF, being an improvement over North American Datum 83 (NAD83), was used as the geodetic reference to process the GPS data.

2.3. Operational Meteorological Observations (Radiosonde and Surface Meteorological Data)

[18] Except for the Valcartier site, radiosonde data provided by the MSC were selected according to their proximity to AEROCAN network stations. Table 1 gives the location of the Sun radiometer and radiosonde sites and the observation period. Valcartier radiosonde measurements

Table 1. Summary of AERONET/AEROCAN Water Vapor 940-nm Band Radiometer and Radiosonde Locations and their Corresponding Observation Period

WVR[a] Site	Nearest Radiosonde Site	Observation Period
Bratt's Lake (50°16′N, 104°42′W)	North Battleford (52°46′N, 108°15′W)	1997–2000
Churchill (5843′N, 94°7'W)	Churchill (58°43′N, 94°7′W)	2000
Kejimkujik (44°22′N, 65°16′W)	Yarmouth (43°52′N, 66°6′W)	1998–2000
Saturna Island (48°46′N, 123°7′W)	Kelowna (49°53′N, 119°29′W)	1999–2000

[a]Water vapor radiometer.

were carried out in collaboration with the meteorological unit of the Defence Research Establishment at Valcartier (DREV) (Quebec, Canada). About 45 radiosondes were launched coincidentally with GPS measurements in Valcartier. The radiosonde signals were processed using the same protocol used by MSC. The pressure and temperature data required for GPS water vapor retrievals were measured using the same sampling frequency and on the same data acquisition system as the GPS.

2.4. Global Environment Multiscale (GEM) Model Data

[19] IWV are also computed using atmospheric profiles from reanalyses using the numerical Global Environment Multiscale (GEM) model of Environment Canada [*Côté et al.*, 1997]. The latter is a highly flexible Canadian modeling system capable of meeting weather-forcasting needs from a global circulation model (GCM). It has also the potential to meet air quality and climate modeling needs. The GEM model has a spatial resolution of 0.33° on the globe ($\sim$37–29 km on the globe) and 28 hybrid levels with three-dimensional finite elements as a spatial discretization method. A time step of 1350 s was used. The data are interpolated horizontally and vertically from the model's 400 $\times$ 200 Gaussian grid for the global data assimilation cycle.

[20] Analyses of atmospheric profiles (pressure, temperature, relative humidity, and wind speed) from the GEM model were completed for the years 1994 and 1997. Summer 1994 data from May to August were considered for the Boreal Atmosphere-Ecosystem Study (BOREAS) sites and June 1997 data for the Sherbrooke site (45°22′N, 71°55′W). The atmospheric profiles were analyzed for 0600 and 1800 UT with ''initial fields'' or ''initial states'' at 0000 and 1200 UT. IWV-NWPM estimates were compared to AEROCAN Sun radiometer network data corresponding to the above sites.

3. Intercomparison and Analysis

[21] In this section, IWV retrieved by the different methods considered are compared. Then, IWV time series are analyzed for several sites across Canada and one site in Alaska. IWV values that represent the overall atmospheric column abundance are expressed in kilograms per squared meter (kg m^2), which is equivalent to precipitable water vapor in millimeters.

3.1. Integrated Atmospheric Water Vapor (IWV) Derived From the Solar Radiometer and the Radiosonde

[22] This section discusses the IWV values derived from the AERONET/AEROCAN Sun radiometer network (IWV-R) and the radiosonde (IWV-S). Table 1 shows the correspondence between radiosonde and Sun radiometer sites in terms of latitude and longitude. The difference in measurement time is <30 min, corresponding to the average time delay to reach the 200-hPa pressure level representing the atmospheric layer below which water vapor in the atmospheric column is contained. Figure 3 shows the scatterplot between IWV-S and IWV-R for selected sites across Canada. Table 2 gives the corresponding linear regression parameters. In the case of Churchill, where both a radiosonde and a solar radiometer were operated at the same site, one can observe good correlation (r^2 coefficient of 99%) in Figure 3a. The other comparisons (Figure 3b) illustrate the influence of the distance between the two sites where instruments are operated, owing to the spatial variability of water vapor concentration. The correlation decreases as the distance between solar radiometer and radiosonde sites increases (Table 2). This highlights the need to consider colocated instruments for comparison purposes. *Wolfe and Gutman* [2000] also report such a linear decrease in correlation coefficients for IWV-GPS versus IWV-S in relation to the distance between the GPS network receiver and radiosonde site.

[23] The Churchill site results, with an RMS difference of $\sim$0.2 (16%) and a mean bias (mb) difference of -1.9 kg m^{-2}, show a systematic overestimate by IWV-R. This relative difference is greater than the 9–10% observed by *Halthore et al.* [1997] with the same radiometer (Cimel) while *Schmid et al.* [1996] found an RMS difference of 1.9 kg m^{-2} (13%) over a 2.5-year period of Sun radiometer and radiosonde observations. In comparison with *Wolfe and Gutman*'s [2000] IWV-R versus IWV-S comparisons, the difference parameters for Churchill (Table 2) are slightly better. The systematic overestimate by the Sun radiometer may be due to a possible drift in radiometer calibration constants, which have an average coefficient of variation (standard deviation/mean) of $\sim$2–4% for the 940-nm channel [*Holben et al.*, 2001]. Furthermore, IWV retrieval from the solar transmittance method is based on the modeling of water vapor transmittance function throughout the 940-nm spectral response of the associated filter. This response may vary from one instrument to another. The accuracy of this modeling, and hence the accuracy of IWV, depends on atmospheric conditions, filter band profile, and position [*Halthore et al.*, 1997]. Furthermore, the resolution of the water vapor spectroscopy has a significant influence on IWV retrieval. In fact, line by line radiative transfer codes such as the Line by Line Radiative Transfer Model (LBLRTM) are more accurate than moderate-resolution (MODTRAN) or low-resolution (LOWTRAN) code in modeling water vapor transmittance [*Schmid et al.*, 1996, 2001]. However, the water spectroscopy remains a source of uncertainty among others. For instance, in a comparison of solar transmittance methods, *Schmid et al.* [2001] found a remaining relative difference of 8% even using the same line by line radiative transfer code, i.e., LBLRTM for the overall solar transmittance considered methods. In this study, the processing was carried out with the corrected and widely used high-resolution transmission molecular absorption (HITRAN-96) database [*Rothman et al.*, 1998; *Giver et al.*, 2000]. The current AERONET procedure for the retrieval of water vapor is based on a transmittance modeling from MODTRAN code that does not include the above-suggested water vapor spectroscopy correction. This procedure can yield accuracies within the generally accepted uncertainty in radiosonde-derived IWV values, i.e., ±10% for narrow band and a newly calibrated Sun radiometer [*Halthore et al.*, 1997].

[24] The procedure used may be improved as a result of recent progress in water vapor spectroscopy. However, the remaining 8% difference found by *Schmid et al.* [2001] despite the spectroscopy correction would suggest more investigations and the evaluation of the above correction

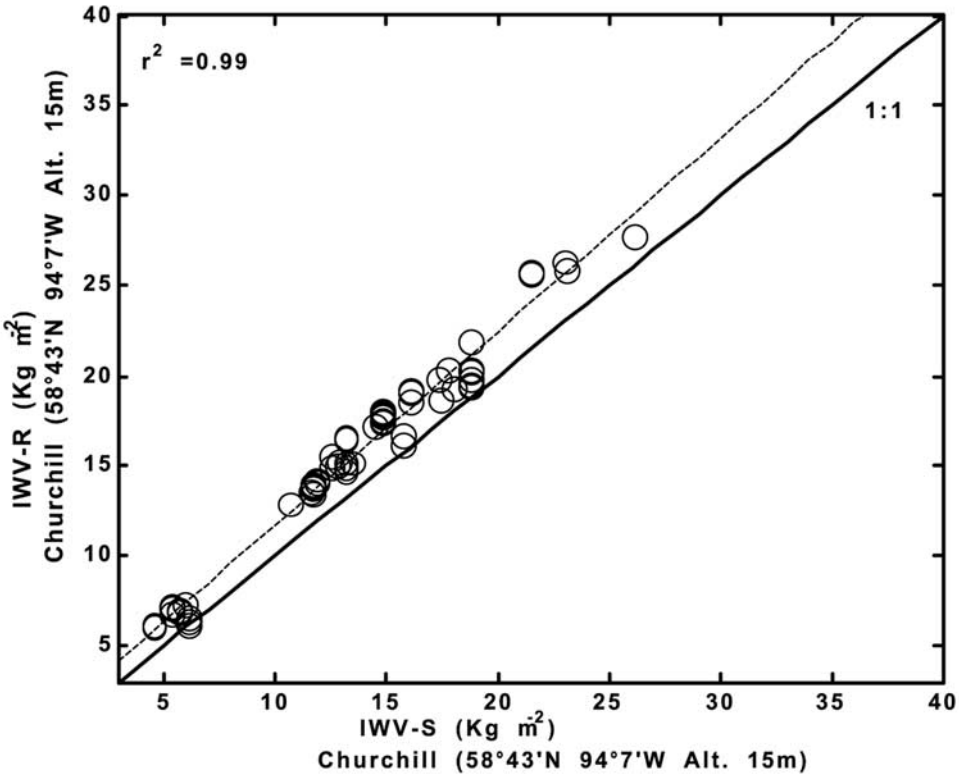

(a) Co-located instruments

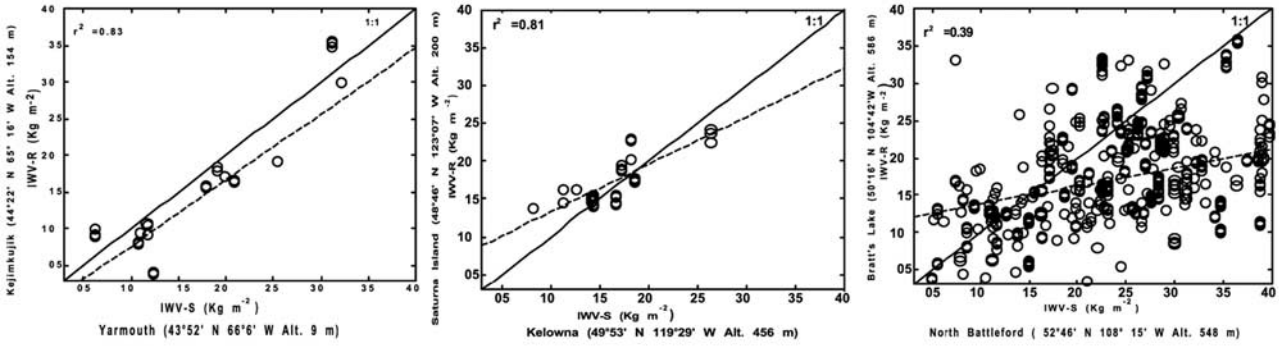

(b) Influence of the distance between instruments

Figure 3. IWV comparison between solar radiometer (R) and radiosonde (S) from various sites across Canada. (a) Water vapor radiometer and radiosonde balloon operated at the same observation locality. (b) Water vapor radiometer and radiosonde balloon separated by a significant distance varying according to localities considered. Note that instruments are not colocated except for the Churchill site.

Table 2. Linear Regression Statistical Parameters for Comparison Between Integrated Water Vapor From Solar Radiometer and Radiosonde Measurements

R Versus S Difference Parameters[a]	Sites			
	Churchill Versus Churchill, Colocation	Kejimkujik Versus Yarmouth	Saturna Island Versus Kelowna	Bratt's Lake Versus Northbattleford
r^2	0.99	0.60	0.25	0.39
Slope	1.07	0.84	0.81	0.24
y intercept, kg m^{-2}	0.9	9.0	6.3	11.4
RMS difference, kg m^{-2}	2.2	6.0	6.9	12.8
Mean bias[b] difference, kg m^{-2}	−1.9	3.0	−0.7	7.6
Maximum, kg m^{-2}	4.1	20.2	3.8	43.4
Minimum, kg m^{-2}	0.1	−4.5	−5.6	−25.6
Standard deviation, kg m^{-2}	1.0	5.2	2.5	10.3
Nobs.[c]	69	32	35	630
Distance between instruments, km	0	108.1	408.3	483.6

[a]R, solar radiometer; S, radiosonde.
[b]mb, mean bias.
[c]Number of observations.

on band-based radiative models such as MODTRAN. This paper is concerned primarily with the validity of the current AERONET/AEROCAN IWV-R retrieval compared to other independent methods. The establishment of a general method that uses recent spectroscopy data free of transmittance modeling error and reduced calibration error remains a next challenge for an accurate retrieval of IWV.

3.2. Validation of IWV-Global Positioning System (GPS) Retrieval

3.2.1. IWV-GPS Versus IWV Radiosonde (IWV-S)

[25] Figure 4 shows the time series and scatterplot for the IWV-GPS and IWV-S comparison. The agreement between the two methods in terms of RMS difference is 1.8 kg m^{-2} with an mb difference of 0.1 kg m^{-2} and a slope of 1.07 (Table 3). Note that the time difference in IWV-GPS and IWV-S measurement points is <30 min, a time difference sufficient to cover the ascent of the radiosonde balloon to an altitude corresponding to a vertical column containing nearly the whole atmospheric water vapor content. This observed IWV/GPS-radiosonde difference is close to the recently published RMS values that vary from 1 to ∼2 kg m^{-2} [*Mätzler et al.*, 2002; *Baker et al.*, 2001; *Niell et al.*, 2001; *Davies and Watson*, 1998; *Tregoning et al.*, 1998] and is less than those reported for regions where precipitable water vapor amounts are larger [*Liou et al.*, 2000; *Ohtani and Naito*, 2000]. *Wade* [1994, 1995] indicates that radiosonde errors can be on the order of 10%, which could explain some of the difference. Errors in IWV-GPS retrieval include orbit precision, receiver noise, pressure sensor errors, the atmospheric parameters used, and multipath errors. Multipath errors should be negligible given the absence of reflective obstacles near our GPS antenna site. According to *Ge et al.* [2000], orbit errors contribute an RMS difference of <6 mm in ZTD estimates (<1 kg m^{-2} in IWV difference) based on comparisons between IGS final orbits and predicted orbits. The phase noise errors due to L1 and L2 frequency linear combination can be considered negligible given the large number of GPS observations (every 30 s). The pressure sensor errors can reach up to ±0.5 kg m^{-2} in IWV. These errors also depend on the amount of water vapor and the low satellite elevation angle (Figure 2). Two other sources of errors are analyzed in sections 3.2.2 and 3.2.3.

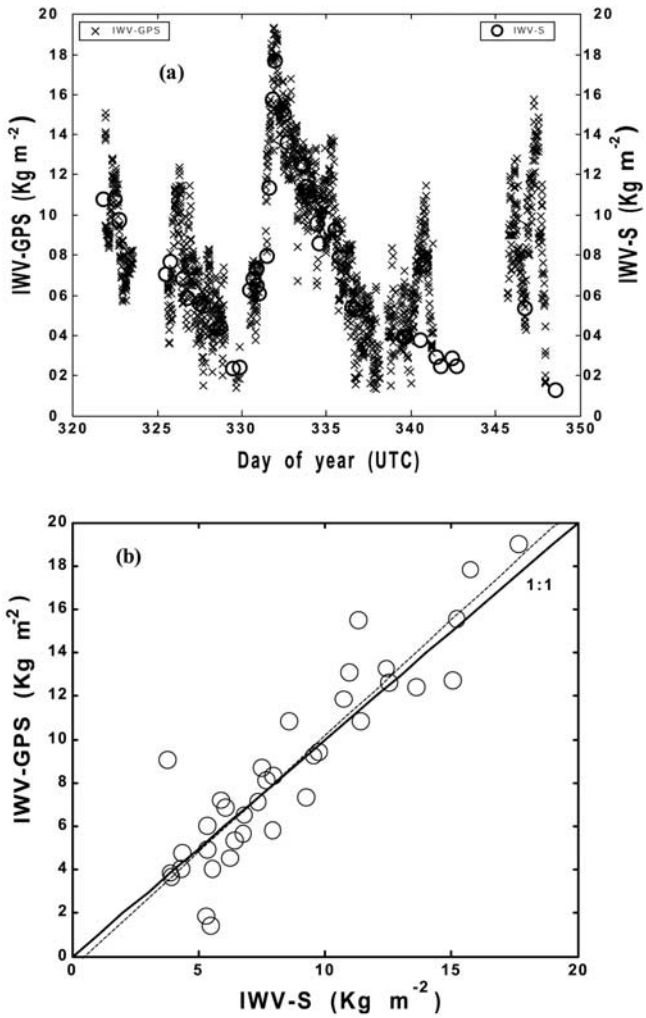

Figure 4. IWV comparison between GPS-derived and radiosonde (S) at the Valcartier site (46°54′N, 71°30′W). Valcartier data range between 16 November and 13 December 2000. (a) Time series and (b) scatterplot for all the points. The IWV points are from instantaneous values. The scatterplot is the result of time synchronization between IWV-GPS and IWV-S with a constraint of time delay <30 min.

Table 3. Difference Parameters for Columnar Integrated Water Vapor Derived From GPS, Radiosonde, and Solar Radiometer Measurements

Method's Intercomparison Difference Parameters	GPS Versus S	GPS Versus R
r^2	0.91	0.92
Slope	1.07	1.05
y intercept, kg m^{-2}	0.5	0.2
RMS difference, kg m^{-2}	1.8	1.9
mb difference, kg m^{-2}	−0.1	−1.0
Maximum, kg m^{-2}	4.0	1.9
Minimum, kg m^{-2}	−5.2	−5.7
Standard deviation, kg m^{-2}	1.8	1.6
Nobs.	36	82

Table 4. Difference Parameters Between the IGS Reference Orbit and Other Orbits[a]

IGS Orbit Versus Other Difference Parameters	JPL	IGR	IGU00	IGU12	NRCan
r^2	0.97	0.97	0.88	0.41	0.99
RMS difference, kg m^{-2}	0.3	0.5	0.8	1.6	0.6
mb difference, kg m^{-2}	0.1	0.4	0.1	−0.3	0.4
Maximum, kg m^{-2}	0.8	1.1	1.9	3.4	1.2
Minimum, kg m^{-2}	−0.6	0.2	−2.2	−3.0	−0.6
Standard deviation, kg m^{-2}	0.3	0.3	0.8	1.6	0.4
Nobs.	95	95	95	95	95

[a]JPL, Jet Propulsion Laboratory International GPS Service (IGS) final orbit; IGR, IGS rapid orbit data; IGU, IGS ultrarapid orbit; NRCan, Natural Resources Canada orbital parameters.

3.2.2. Sensitivity to GPS Satellite Orbit

[26] Figure 5 highlights the sensitivity of IWV-GPS retrieval to various satellite orbit characteristics using the November records for Sherbrooke as an example. The IGS precise final orbit, which has an ephemeris accuracy of $<\pm 0.05$ m and clock accuracy of ± 0.1 ns [*IGS*, 2002; *Collins et al.*, 2002], was chosen as the reference orbit. These data are available 2 weeks after GPS observations [*Neilan et al.*, 1997; *Kouba et al.*, 1998]. The difference parameters between the reference and the other orbits that are available in close to real time are shown in Table 4. The IGR from IGS orbits and clock products called "rapid orbit data" are available with about a 17-hour delay after the observations and have an accuracy of about ±0.05 m (ephemeris) and ±0.2 ns (clock). The ultrarapid (IGU00 and IGU12) combinations are generated twice each day by IGS and contain 48 hours' worth of orbits; the first 27 hours are based on observations, and the last 21 hours are predicted orbits. The accuracy associated with these orbits is about ±0.25 m (ephemeris) and ∼±5 ns (clock). Natural Resources Canada (NRC) orbit and clock data are computed from a global GPS network. The expected accuracy is ±0.05 m for final orbit and ±0.06 to ±0.088 m for ultrarapid orbit with ±0.1 and ±0.2 ns as clock accuracies, respectively [*Collins et al.*, 2002].

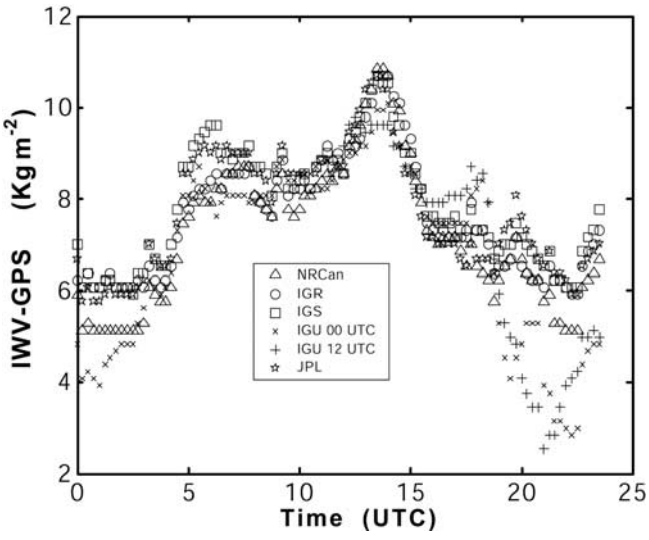

Figure 5. Sensitivity of IWV-GPS retrieval to GPS satellite constellation. JPL, Jet Propulsion Laboratory IGS final orbit; IGR, International GPS Service (IGS) rapid orbit data; IGU, IGS ultrarapid orbit, Natural Resources Canada (NRCan) orbital parameters. The IWV values are computed with a surface pressure of 1013 hPa and a surface temperature of 5°C.

[27] Our results show that the JPL final orbit and the IGR orbits give the best agreement compared to IGS (reference) with RMS differences of 0.3 kg m^{-2} and ±0.5 kg m^{-2}, respectively. Note that JPL refers to NASA JPL's computation of IGS final orbits and clock products. The availability of accurate GPS constellation satellite orbits and clock data in near real time could improve meteorological forecasts by using columnar water vapor amounts from the GPS network. However, in practice, only the IGU 24-hour predicted orbit data are readily available on a regular basis. *Baker et al.* [2001] show that the removal of low-accuracy satellite orbits in 24-hour predicted files significantly improves the IWV-GPS retrieval to reach an accuracy close to the one obtained using IGS precise orbits, i.e., about ±1 kg m^{-2}. For IWV analysis in postprocessing mode from a single-unit GPS system, IGS final orbit and clock parameters remain the only alternative for maximum accuracy in IWV-GPS retrievals.

[28] The IWV RMS differences reported in Table 4 are in the range of GPS meteorology errors reported by *Rocken et al.* [1993]. Investigations are being carried out by several institutions [*Muellerschoen et al.*, 2000; *Reigber et al.*, 2002] including the Geodetic Survey Division of Natural Resources Canada to compute near-real-time precise orbits and clock data for meteorological purposes using GPS.

3.2.3. Sensitivity to Meteorological Parameters

[29] IWV retrievals from GPS meteorology depend mainly on atmospheric temperature, relative humidity, and pressure as revealed by several empirical relationships [*Leckner*, 1978; *Garrison and Adler*, 1990; *Gueymard*, 1994]. One of the most important variables in the GPS meteorology approach is the weighted mean atmospheric temperature [*Davis et al.*, 1985], which allows the conversion of the zenith wet delay into IWV. This parameter (see Appendix A) can be computed from radiosonde or numerical simulation profiles (pressure and temperature) or from surface temperature using a linear regression [*Bevis et al.*, 1992]. The regression parameters vary according to location and season [*Bevis et al.*, 1992; *Davies and Watson*, 1998; *Liou et al.*, 2000]. Furthermore, the weight-

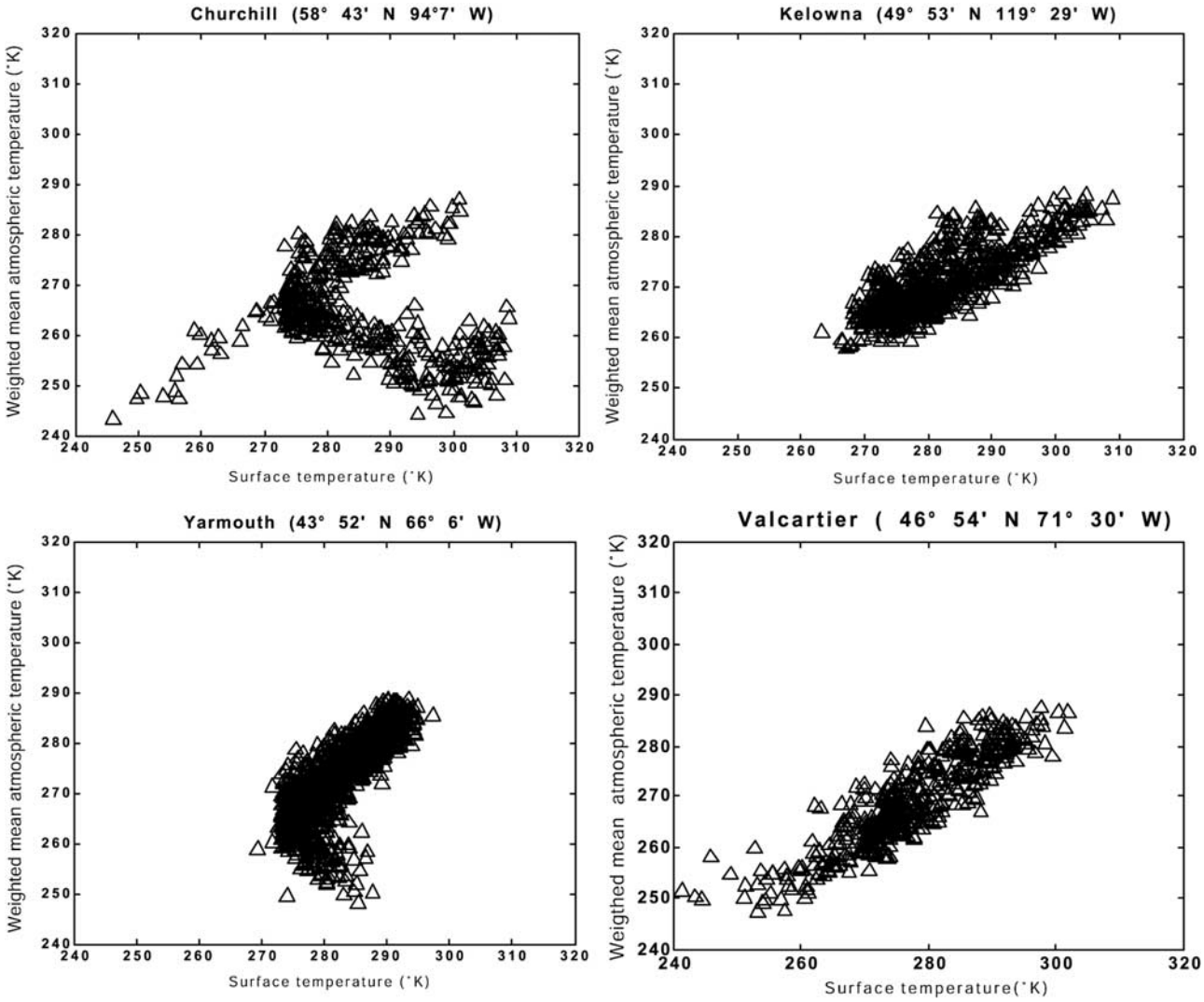

Figure 6. Weighted mean atmospheric temperature (T_m) versus surface Temperature (T_s) for various localities in Canada. The T_m calculations are based on upper air radiosonde data according to the *Davis et al.* [1985] relationship.

ed mean atmospheric temperature can be estimated from a modeling approach [*Ingold et al.*, 1998; *Mendes et al.*, 2000].

[30] Figure 6 shows graphs of weighted mean atmospheric temperature (T_m) obtained from radiosondes and surface temperature (T_s) for selected Canadian sites (Table 1, $\geq$400 observations for each site according to radiosonde by radiosonde processing). In the case of the Kelowna and Valcartier sites, T_m is linearly proportional to T_s, whereas both positive and negative slopes were observed for the Churchill and Yarmouth sites. The negative slope is linked to an inversion in temperature profile where temperature increases with altitude in the troposphere. These inversions are characteristic of the Arctic climate system [*Hoff*, 1988; *Bokoye et al.*, 2002] and may occur at lower latitudes that come under the influence of Arctic air masses in the winter season (e.g., Yarmouth). The separation limit in temperatures between the normal profile and the inversion profile is $\sim$260 K, which corresponds to a potential isothermal atmospheric temperature also observed by *Hoff* [1988]. Furthermore, a temperature inversion that corresponds to stable atmospheric conditions in the troposphere can also be part of the daily meteorological cycle (from sunset to just before sunrise in windless to low-wind conditions).

[31] This illustrates that the usual linear relationships between T_m and T_s [*Bevis et al.*, 1992; *Davies and Watson*, 1998; *Liou et al.*, 2000] are not appropriate for GPS meteorology in areas influenced by Arctic air masses. A better knowledge of the atmospheric temperature profile during GPS observations is required for these cases. The error introduced by an incorrect mean temperature can be on the order of 20% [*Bevis et al.*, 1992, 1994] in the IWV to zenith wet delay ratio (see Appendix A). However, in the framework of meteorological forecasting using GPS observations the above conversion is not always necessary as the models can assimilate directly the total slant or zenith delays [*MacDonald et al.*, 2002; *Yang et al.*, 1999; *Kuo et al.*, 1993, 1996], allowing the models to partition the wet and dry components.

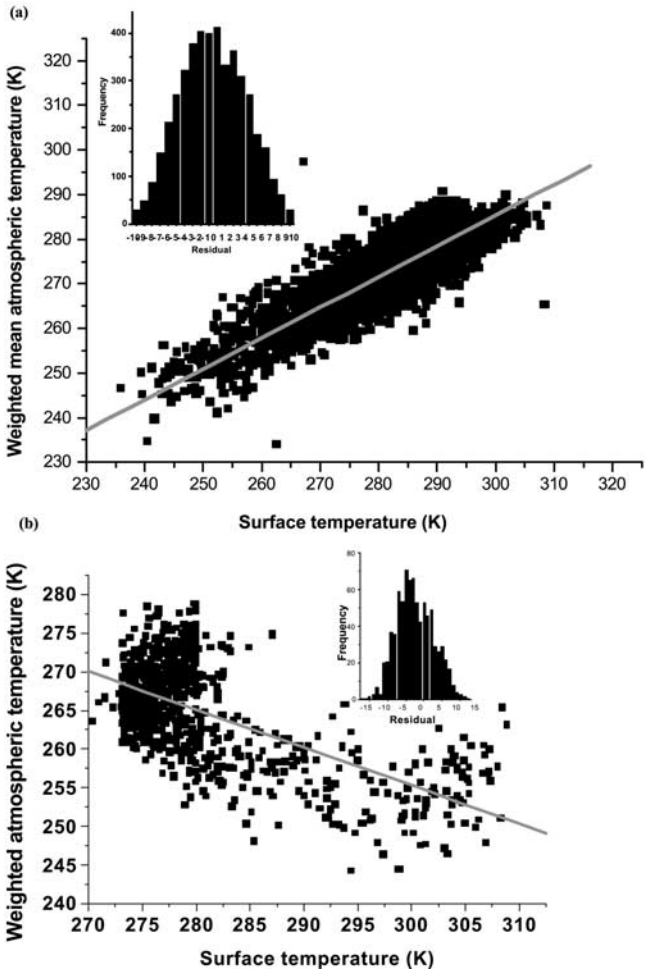

Figure 7. Linear regression between T_m and T_s. (a) Positive slope, $T_m = (0.69 \pm 0.01)T_s + (78.92 \pm 1.76)$. T_m increases as T_s increases relationship obtained from 4603 radiosondes corresponding to standard atmospheric profiles with correlation cofficient $r = 0.85$. (b) Negative slope, $T_m = (-0.49 \pm 0.02)T_s + (402.56 \pm 5.77)$. T_m decreases as T_s increases from 830 upper air profiles with temperature inversion in the troposphere with $r = 0.64$. In both cases the histogram of the residuals are shown and the upper air records from various Canadian sites considered cover the period 1998–2000. Note that both T_m and T_s are expressed in Kelvin units.

[32] The linear regression between T_m and T_s with a positive slope was established from 4603 radiosondes for four different sites across Canada (Table 1) from 1997 to 2000. This regression corresponds to the large-scale trend in the atmosphere where temperature decreases with height. Note that only atmospheric profiles excluding temperature inversions were considered in the above regression.Figure 7a shows the corresponding scatterplot of T_m versus T_s with associated residuals. Table 5 gives our regression parameters compared to those of *Bevis et al.* [1992], which are not significantly different. Results reported by *Liou et al.* [2000] and *Davies and Watson* [1998] for regional studies are slightly different (with an RMS difference of ~2 K). *Mendes et al.* [2000] found an RMS difference of 3.1 K from T_m comparisons between models and observation. Some T_m-related RMS differences ranging between 3 and 5 K were retrieved by *Ingold et al.* [1998] at various altitudes from millimeter wave propagation. Our regression parameters were used to compute IWV in this study.

[33] In Figure 7b, T_m versus T_s linear regression in the case of temperature inversion in the troposphere was plotted from 830 upper air profiles. The regression results in a correlation coefficient r of 0.64 and an RMS difference of 5.02 K, whereas $r = 0.85$ and RMS difference is 4.31 in the noninversion case (Figure 7a). The residual histogram shown in the right corner of Figure 7b presents an asymmetry compared to that of Figure 7a.

3.2.4. Solar Radiometer and GPS-Derived IWV

[34] Figure 8 shows the time series and the linear regression for the IWV-R and IWV-GPS comparison. Note that the solar radiometer data in the 940-nm band were cloud screened [*Smirnov et al.*, 2000]. The time series shows good agreement between the two methods, with similar peak-to-peak daily cycles (Figure 8a). As also suggested by *Bouma and Stoew* [2001], the GPS approach appears to be a useful tool for monitoring high-frequency daily IWV variations. A linear regression using 82 points when the observation time was synchronized to within 30 min gives differences of 1.92 kg m^{-2} RMS and −1.0 kg m^{-2} mb (Table 3). The linear regression shows an overestimation trend for IWV-R values that can be linked to the presence of systematic errors for this solar radiometer. *Mätzler et al.* [2002] calculated slope and mb differences of 1.08 and −0.57 kg m^{-2}, respectively, for a similar comparison using a GPS receiver and the 946-nm band Sun radiometer data. These results were obtained with Sun radiometer data available only at noon for comparison with radiosonde data at 1200 UT. Note that the error in Sun radiometry is a decreasing function of solar elevation angle and this explains the best mb difference. *Sierk et al.* [1997] compared the IWV from a GPS receiver and a solar spectrometer operating in the near-infrared region using high-resolution absorption band measurements over a 30-day period and reported differences of −3.7 kg m^{-2} mb and an RMS and ~4 kg m^{-2} RMS. For all these studies the differences observed between the solar radiometer and the GPS are in the range of other comparisons (GPS-radiosonde and GPS-microwave radiometry [e.g., *Niell et al.*, 2001; *Tregoning et al.*, 1998; *Duan et al.*, 1996; *Elgered et al.*, 1991, 1995]). The

Table 5. Linear Regression Parameters for the Relationship Between Weighted Mean Atmospheric Temperature and Surface Temperature[a]

T_m Versus T_s Linear Regression Parameters[b]	*Bevis et al.* [1992]	This Paper
Slope	0.72	0.69
y intercept, K	70.2	78.9
RMS difference, K	4.7	4.3
	8718	4603
	USA, multiyear	Canada, multiyear

[a]Given by *Bevis et al.* [1992] compared to our analysis. For comparison needs our regression does not include any radiosonde data corresponding to an inversion in temperature profile.

[b]T_m, weighted mean atmospheric temperature; T_s, surface temperature.

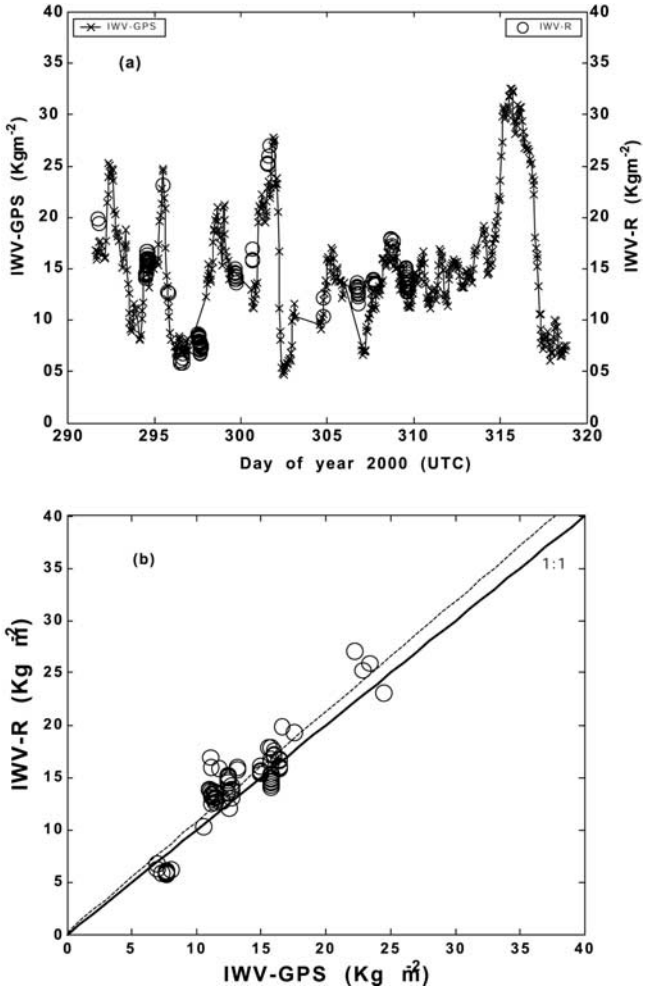

Figure 8. IWV comparison between 940-nm solar band Radiometer (R) and GPS derived at Sherbrooke site (45°22′N, 71°55′W) for the period from October to November 2000. (a) Time series and (b) scatterplot for all the points. The IWV points are for instantaneous values. The scatterplot is the result of time synchronization between IWV-GPS and IWV-R with a constraint of time delay <30 min.

observed IWV-R data slightly exceed IWV-GPS estimates. Assuming IWV-GPS as the reference, the observed RMS difference of 1.9 kg m^{-2} may be linked to calibration drift in the radiometer data owing to possible optical alteration (filter aging [*Halthore et al.*, 1997; *Holben et al.*, 1998]) and/or uncertainties in the 940-nm band solar transmittance computation [*Schmid et al.*, 1996, 2001]. Moreover, the atmospheric composition in the viewing direction of the radiometer toward the Sun may be different from the "view" of the GPS receiver (Figure 2). Recent research, by *Baker et al.* [2001], *Guerova et al.* [2001], *Ware et al.* [2000], *Gutman and Benjamin* [2001], and *Wolfe and Gutman* [2000], has shown the advantage and the high potential of GPS meteorology for IWV monitoring with an accuracy ranging between ±1 and ±2 kg m^{-2} under all weather conditions with minimum technical support.

[35] Instrument calibration problems may be a limitation for long term water vapor monitoring using Sun radiometry. However, the comparison between IWV-GPS and 940-nm solar radiometer with an RMS of ±1.9 kg m^{-2} allows the establishment of a useful IWV emerging climatology. Maintaining a water vapor radiometer network like AERONET remains a big challenge with respect to routine operations such as calibration, data processing, quality assurance, and logistical support. The possibility of monitoring the outputs of this network accurately using a single GPS unit at several reference sites improves the quality assurance of the network.

4. A Sun Radiometer Water Vapor Database

4.1. Interannual Summer Spatial and Temporal Water Vapor Variability

[36] Table 6 highlights the spatial and temporal distribution of summer (June, July, and August) IWV-R from Sun radiometry in Canada and Alaska over the period of data availability for each site from 1994 to 2001. The nine sites studied are classified according to decreasing latitude, which is associated with mean increasing water vapor from 17 kg m^{-2} in the Arctic to 23 kg m^{-2} in southern Canada (Kejimkujik, Nova Scotia, Canada). The average summer value for all the sites is 19.8 ± 6.1 kg m^{-2}. The standard deviation, which can reach ∼30% of the mean summer values, demonstrates the high variability of water vapor amount during the summer period. There is no obvious year to year trend for any of the sites (Table 6), in contrast with a study of water vapor trends for North America based on radiosonde measurements from 1973 to 1993, which showed an increase in precipitable water over all regions with the exception of slight decreases in northern and eastern Canada [*American Geophysical Union*, 1995]. Note that the number of observations (Table 6) is significantly different across time and space.

[37] Figure 9 shows the mean summer month values from Sun radiometry over the last 8 years (1994–2001) for the Bonanza Creek, Alaska, and Waskesiu (Saskatchewan, Canada) sites. In Bonanza Creek (64°44′N, 148°18′W), the 1994–2001 average (16.6 ± 4.9 kg m^{-2}) is in the range of the summer (June, July, and August) mean values of Environment Canada's aerology (upper air observations) normals (1971–2000) as computed for four northwestern Canadian sites in the same area. These upper air normals correspond to more than 800 radiosonde flights per month between the surface and a pressure level of at least 50 hPa. The individual sites for these normals are Fort Smith (60°02′N, 111°56′W), 20.0 ± 1.7 kg m^{-2}; Inuvik (68°19′N, 133°31′W), 17.1 ± 1.8 kg m^{-2}; Norman Wells (65°17′N, 126°45′W), 19.4 ± 1.8 kg m^{-2}; and Whitehorse (60°44′N, 135°04′W), 17.0 ± 1.8 kg m^{-2}. Combining these values gives a regional precipitable water value of 18.8 ± 2.2 kg m^{-2} (denoted by a solid horizontal line in Figure 9). The mean summer value for Bonanza Creek is 16.6 ± 4.9 kg m^{-2} computed from 5517 observations. The regional IWV monthly means computed from the above normals for June, July, and August are 16.3 ± 1.5, 20.1 ± 1.4, and 18.9 ± 1.5 kg m^{-2}, respectively. The number of radiosondes (0000 and 1200 UT) considered for each monthly normal is >800 between surface pressure and 50 hPa. Similar summer monthly means were reported by *Gueymard* [1994] for 24 Canadian sites for the period 1961–1970 and by *Serreze et*

Table 6. Multiyear Summer Observations of Atmospheric Water Vapor for Different Sites in Canada and Alaska[a]

Site/Latitude	1994		1995		1996		1997		1998		1999		2000		2001		Mean All Period	
	IWV	Nobs.	IWV	Nobs.	IWV	Nobs.	IWV	Nobs.	IWV	Nobs.	IWV	Nobs.	IWV	Nobs.	IWV	Nobs.	IWV	Nobs.
Barrow, 71.30°							15.9 ± 4.3	54			17.3 ± 4.5	431					16.8 ± 4.7	550
Bonanza Creek, 64.73°	23.1 ± 5.2	365	16.7 ± 3.1	607	13.9 ± 3.7	956	21.4 ± 5.2	232	17.9 ± 4.8	491	15.9 ± 4.8	1290	16.0 ± 3.8	909	12.0 ± 5.8	667	16.6 ± 4.9	5517
Thompson, 55.78°	17.0 ± 5.0	471	13.9 ± 5.3	741	16.9 ± 4.4	1436	20.8 ± 5.4	1011	21.8 ± 6.9	915	10.8 ± 5.2	835			17.2 ± 3.4	131	18.3 ± 6.0	5540
Waskesiu, 53.92°	16.8 ± 4.7	1210	16.7 ± 4.5	972	16.2 ± 3.8	1514	20.8 ± 4.7	1534	20.8 ± 5.6	1711	20.8 ± 5.5	470	17.9 ± 7.2	2499	19.6 ± 4.3	1619	18.8 ± 5.1	11529
Bratt's Lake, 50.26°							19.9 ± 4.8	1362			20.0 ± 5.2	967	19.0 ± 6.1	678	20.6 ± 5.4	1871	20.1 ± 5.3	4878
Saturna Island, 48.77°											21.2 ± 4.9	624	21.5 ± 4.1	422	21.1 ± 4.1	1837	21.2 ± 4.3	2883
Sherbrooke, 45.37°			18.0 ± 7.2	2178			20.0 ± 5.8	1636	20.3 ± 6.3	410	23.5 ± 6.7	1601	25.2 ± 5.6	354	23.5 ± 7.3	1553	21.1 ± 7.2	7732
Kejimkujik, 44.37°									25.3 ± 8.7	182	21.9 ± 6.4	135	19.0 ± 5.7	81			22.8 ± 7.8	398
Egbert, 44.1°							21.4 ± 4.8	194	21.7 ± 6.3	1271	24.0 ± 6.7	1259	20.9 ± 5.9	1306	22.8 ± 6.3	1727	22.4 ± 6.3	5757

[a]Years are 1994–2001; summer months are June, July, and August. Mean values of IWV ± standard deviation are expressed in kg m^{-2}. Nobs. is given for each year considered. IWV, integrated atmospheric water vapor.

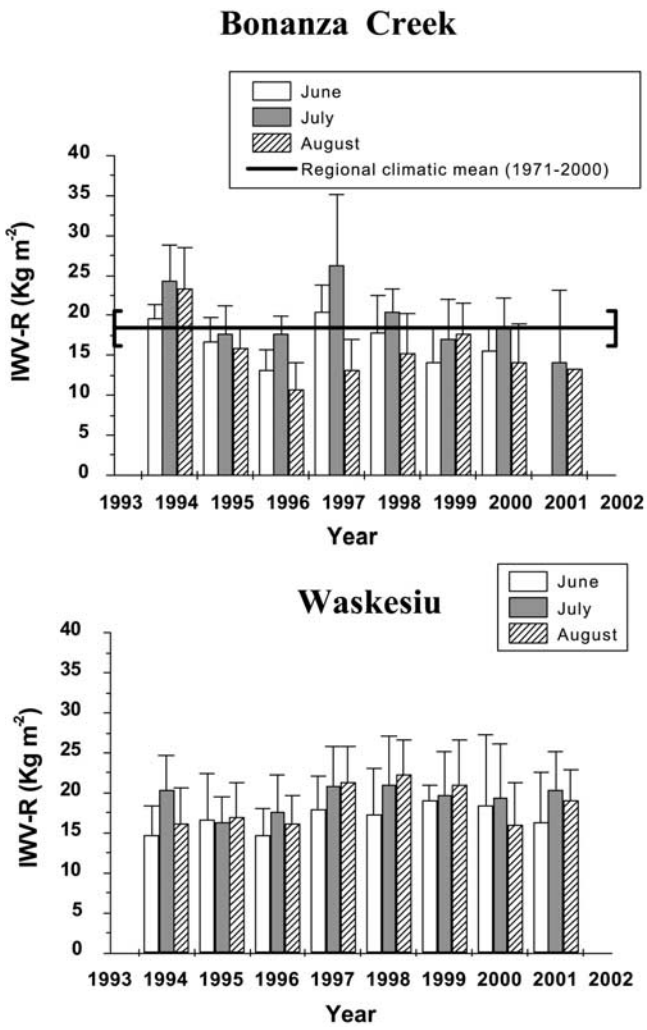

Figure 9. Eight years of monthly summer (June, July, and August) means Sun radiometer observation of atmospheric water vapor at Bonanza Creek (64°44′N, 148°18′W) and Waskesiu (53°55′N, 106°04′W) sites. The solid horizontal line represents radiosonde summer climatological normal value which is computed from normal atmospheric profiles (1971–2000) of the following Northwest Canadian sites close to the Bonanza Creek site: Fort Smith (60°02′N, 111°56′W), Inuvik (68°19′N, 133°31′W), Norman Wells (65°17′N, 126°45′W), and Whitehorse (60°44′N, 135°04′W).

al. [1994] using data from 1954 to 1990, which includes rawinsonde records for stations over 65°N. Slight interannual variations are observed at Bonanza Creek, possibly driven by forest fire occurrences [*Kasischke et al.*, 1993; *Markham et al.*, 1997], while the peak in 1997 may be linked to the El Niño event [*Latif et al.*, 1995] observed the same year [*Daifong and Philander*, 1997; *Hoerling and Kumar*, 1997; *Prabhakara et al.*, 1985; *Webster and Palmer*, 1997].

4.2. Global Environmental Model Validation Using Sun Radiometry

[38] We compare in this section IWV time series values from solar radiometer and numerical weather prediction model (NWPM) outputs from the GEM modeling system. Figure 10 displays the IWV-NWPM versus IWV-R com-

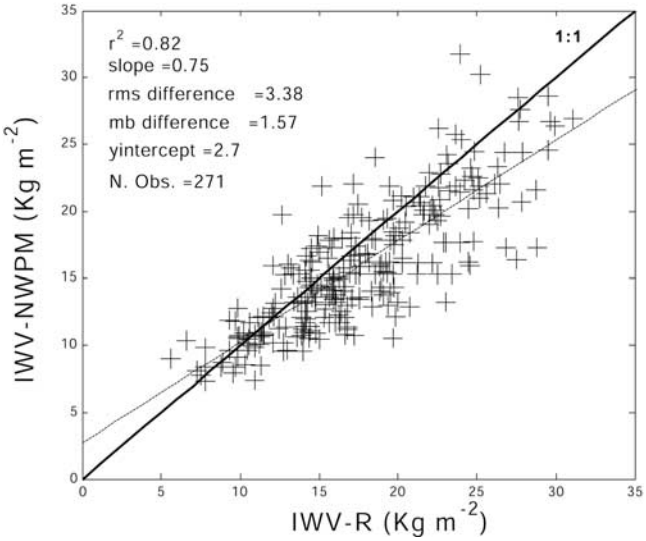

Figure 10. IWV comparison between 940-nm solar band radiometer (R) and the reanalysis of the Canadian numerical weather prediction model (NWPM). The data are compiled from the Sherbrooke site (45°22′N, 71°55′W) and the following BOREAS sites in the provinces of Saskatchewan and Manitoba: Thompson (55°47′N, 97°50′W), Waskesiu (53°55′N, 106°04′W), Northern Study Area (NSA) (53°40′N, 104°39′W), and Southern Study Area (SSA) (55°54′N, 88°17′W).

parison for data compiled from various sites. The comparison shows that between radiometer observations and the forecast model (r^2 = 0.82, RMS difference is 3.4 kg m^{-2}, mb difference is 1.6 kg m^{-2}), there is a slight underestimation of IWV-NWPM, in particular for high IWV values (see dashed regression line in Figure 10). Note that the site-to-site comparisons (not shown here) did not reveal any local dependency, which suggests systematic errors.

[39] The above errors, similar to those observed by others [*Yang et al.*, 1999; *Bevis et al.*, 1996], may be due to radiometer calibration or errors generated by the model. Numerical weather forecasts are always initialized, i.e., the establishment of spatial structure of the atmosphere at a specific time or epoch (at 0000 or 1200 UT) using radiosonde profiles. Thus radiosonde uncertainties should affect the error budget related to IWV-NWPM. Moreover, radiosonde observation measurements were performed generally twice per day, at 0000 and 1200 UT. The weather forecast model produces predictions from reanalysis data or initial "fields" at 0000, 0600, 1200, and 1800 UT. *Bevis et al.* [1996] report that the upper boundary on the ZWD RMS prediction error is roughly 0.01 m (equivalent to ~1.67 kg m^{-2} in IWV) plus 10% of predicted ZWD if the latter lies between 0 and 0.2 m (or ~33.4 kg m^{-2} in IWV). In a similar comparison between reanalysis (from a fine resolution numerical weather prediction model) and radiosonde-derived IWV, *Yang et al.* [1999] found an RMS difference ranging from 1.3 to 2.4 kg m^{-2} and an mb difference of −1.4 kg m^{-2} to 0.8 kg m^{-2} for four sites in Sweden and Finland. Models can also be used to forecast IWV; however, according to *Bevis et al.* [1996] and *Yang et al.* [1999], the error in forecasting ZWD, and therefore IWV, from numerical weather prediction increases with integration time (between two initial "fields") and the magnitude of IWV.

5. Summary and Outlook

[40] Integrated water vapor in the atmosphere has been analyzed using the following four alternative methods: radiosonde (IWV-S), solar radiometry (IWV-R), forecast model (IWV-NWPM), and GPS meteorology (IWV-GPS). This multisensor comparison highlights the importance of problems related to the determination of integrated water vapor amounts. The comparison results suggest an overestimation by the 940-nm band of the radiometer. The efficiency of GPS meteorology for water vapor monitoring clearly appears promising, except for the problems associated with estimating weighted mean atmosphere temperature. The ability of the GPS software from the Geodetic Survey Division of Natural Resources Canada to retrieve columnar water vapor amounts with an accuracy (RMS) of less than ±2 kg m^{-2} as compared to radiosonde data has been demonstrated. From a comparison of tropospheric zenithal delay estimates over four Canadian sites, *Collins et al.* [2002] have shown that GPSpace gives an RMS agreement of ~±1.7 kg m^{-2} in IWV to that calculated by JPL's GPS-Inferred Positioning System and Orbit Analysis Simulation Software (GIPSY-OASIS). Furthermore, in comparison to Sun radiometry, GPS meteorology is potentially more appropriate for monitoring water vapor in Arctic regions where there are months when the sun is absent or nearly so. The summer water vapor climatology derived from the AERONET/AEROCAN Sun radiometer network for different sites in Canada and Alaska shows spatial and interannual variations ranging between 13 and 23 kg m^{-2}.

[41] Compared to Sun radiometry, GPS may provide better temporal resolution of IWV because of lower costs (user segment) and since it is a stable monitoring system that requires little attention once established at a location. GPS meteorology appears to be a key method for future water vapor monitoring, in particular for severe high-latitude climate areas once the problems associated with mean atmospheric temperature can be resolved.

Appendix A

[42] The tropospheric delay is described as the product of zenith total delay (ZTD) and the mapping function [*Niell*, 1996], which depends on the satellite elevation angle. In this study, ZTD is estimated together with geodetic parameters such as station positions and clock errors of GPS receivers by an overall least squares inversion technique [*Kouba and Héroux*, 2001; *Collins et al.*, 2002]. ZTD can be partitioned into wet delay (ZWD) and hydrostatic delay (ZHD)

$$\mathrm{ZTD} = \mathrm{ZWD} + \mathrm{ZHD}.$$

Both of these delays are the smallest for paths in the zenith direction and increase approximately inversely with the sine of elevation angle. The mapping function describes the dependence on the elevation angle [*Davis et al.*, 1985].

[43] The typical value of ZHD is ~2.3 m at sea level in the zenith direction and represents 90% of the ZTD. The

value of the zenith wet delay can be <0.1 m in arid regions or during the winter and ~0.4 m in humid areas or during the summer.

[44] ZHD can be modeled simply [*Saastamoinen*, 1972] as a function pressure profile and the mean value of gravity in the column of the atmosphere. The latter can be accurately evaluated in terms of height Z (in meters) and latitude φ (in degrees) of ground point of which the altimeter measurement is made. Thereafter, *Elgered et al.* [1991] showed that ZHD can be evaluated from the surface pressure with an accuracy better than ±1 mm. The surface pressure must be accurate to at least ±0.3 hPa in this case. Both previous contributions lead to

$$\mathrm{ZHD} = \frac{(2.2779 \pm 0.0024)P_s}{1 - 0.00266\ \cos 2\varphi - 0.00028\ Z},$$

where P_s is the total pressure in hPa at the Earth's surface. The latter was measured in parallel with GPS observations (i.e., with the same temporal resolution of 30 s) by means of the Campbell Scientific barometric pressure sensor (model 61202), which has an operating range of 600–1100 hPa. The associated accuracy is ±0.3 hPa at 20°C. Finally, the integrated water vapor (IWV) can be computed by the following equation [*Bevis et al.*, 1994]:

$$\mathrm{IWV} = k\mathrm{ZWD},$$

where

$$k = \frac{10^8}{\rho R_v \left[\left(\frac{k_3}{T_m}\right) + k_2'\right]}.$$

ρ is the water vapor density (in kilograms per cubic meter (kg m^3)), R_v is the specific gas constant of water vapor (J/Kg − K), k'_2 is 22.1 ± 2.2 (in Kelvin per hectopascal (K/hPa)), k_3 is (3.739 ± 0.012) × 10^5 (K^2/hPa), T_m is the weighted mean temperature of the atmosphere (K) expressed by *Davis et al.* [1985] as follows:

$$T_m = \frac{\int \frac{P_v}{T} dz}{\int \frac{P_v}{T^2} dz},$$

where P_v is the partial pressure of water vapor (in hectopascals) and T is the temperature of the atmosphere (K) at a level z.

[45] According to this paper, T_m can be estimated from the surface temperature in the Canadian context as

$$T_m = 0.69T_s + 78.92.$$

In our work, T_s was measured in parallel to GPS observations using a Campbell Scientific CS500 temperature sensor that covers the range −40°C to +60°C. Its accuracy is ±0.3°C at 0°C.

[46] **Acknowledgments.** We wish to thank the Geodetic Survey Division of Natural Resources Canada, in particular Pierre Tétreault, for allowing us to use the geodetic software GPSpace. The authors are grateful to John R. Vande Castle (Department of Biology, University of New Mexico), the principal investigator of the AERONET site at Bonanza Creek, for his authorization to use the data from this site. The authors wish to thank Brent Holben and all AERONET staff at the National Aeronautics and Space Administration (NASA) Goddard Space Flight Center (GSFC) for the constant logistical support and their partnership, Natural Sciences and Engineering Research Council of Canada (NSERC), the Canadian Institute for Climate Studies (CICS), the Meteorological Service of Canada (MSC) of Environment Canada, the Canada Centre for Remote Sensing (CCRS), the Quebec Fonds pour la Formation de Chercheurs et d'Aide à la Recherche (FCAR) that provided GPS equipment, the Manitoba Northern Research Fund Program, and the Churchill Northern Studies Center (CNSC) for their contribution to the AEROCAN project. We are grateful to J. Freemantle of York University for his help in the framework of AEROCAN activities. Thanks go to the aerological section of Defence R and D Canada, Valcartier, in particular Patrice Tremblay for providing radiosonde data in Valcartier. Also, many thanks go to Monique Lapalme of the Climate Archives Department of Environment Canada for providing climatic normal profiles for several northern Canadian sites. We acknowledge the comments of Godelieve Deblonde of Environment Canada (Dorval, Quebec), which have improved the paper.

References

American Geophysical Union, Water vapor in the climate system, *Spec. Rep.*, Washington, D.C., 1995.

Baker, H. C., A. H. Dobson, N. T. Penna, M. Higgins, and D. Offiler, Ground-based GPS water vapor estimation: Potential for meteorological forecasting, *J. Atmos. Sol. Terr. Phys.*, *63*, 1305–1914, 2001.

Bevis, M., S. Businger, T. A. Herring, C. Rocken, R. A. Anthes, and R. H. Ware, GPS meteorology: Remote sensing of atmospheric water vapor using the Global Positioning System, *J. Geophys. Res.*, *97*(D14), 15,787–15,801, 1992.

Bevis, M., S. Businger, T. A. Herring, R. A. Anthes, C. Rocken, and R. H. Ware, GPS meteorology: Mapping zenith wet delay onto precipitable water, *J. Appl. Meteorol.*, *33*, 379–386, 1994.

Bevis, M., S. Chiswell, S. Businger, T. A. Herring, and Y. Bock, Estimating wet delays using numerical weather analyses and predictions, *Radio Sci.*, *31*, 477–487, 1996.

Blanchet, J.-P., and E. Girard, Arctic greenhouse cooling, *Nature*, *371*, 383, 1994.

Blanchet, J.-P., and E. Girard, Water-vapor temperature feedback in the formation of continental Arctic Air: Implications for climate, *Sci. Total Environ.*, *160*/*161*, 793–802, 1995.

Bokoye, A. I., A. Royer, N. T. O'Neill, G. Fedosejevs, P. M. Teillet, L. J. B. McArthur, and P. Cliche, Characterization of atmospheric aerosols across Canada from a ground-based Sun radiometer network: AEROCAN., *Atmos. Ocean*, *39*(4), 429–456, 2001.

Bokoye, A. I., A. Royer, N. T. O'Neill, and L. J. B. McArthur, A North American Arctic aerosol climatology using ground-based sunphotometry, *Arctic*, *55*(3), 215–228, 2002.

Bouma, H. R., and B. Stoew, GPS observations of daily variations in the atmospheric water vapor content, *Phys. Chem. Earth, Part A*, *26*(6–8), 389–392, 2001.

Collins, P., Y. Mireault, and P. Héroux, Strategies for Estimating Tropospheric Delays with GPS, *Proc. IEEE Position Location and Navig. Symp.*, pp. 120–127, Nat. Resour. Can. Geodetic Surv. Div., Ottawa, Ontario, Canada, 2002.

Côté, J., J. G. Desmarais, S. Gravel, A. Méthot, A. Patoine, M. Roch, and A. Staniforth, The operational CMC/MRB Global Environmental Multiscale (GEM) model, *Rep. Atmos. Environ. Service*, 58 pp., Environ. Can., Dorval, Quebec, 1997.

Curry, J. A., J. L. Schramm, M. C. Serreze, and E. E. Ebert, Water vapor feedback over the Arctic Ocean, *J. Geophys. Res.*, *100*(D7), 14,223–14,229, 1995.

Daifong, G., and S. G. Philander, Interdecadal climate fluctuations that depend on exchanges between tropics and extratropics, *Science*, *275*(7), 805–807, 1997.

Davies, O. T., and P. A. Watson, Comparisons of integrated precipitable water-vapor obtained by GPS and radiosondes, *Electronics Lett.*, *34*(7), 645–646, 1998.

Davis, J. L., T. A. Herring, I. I. Sapiro, A. E. E. Rogers, and G. Elgered, Geodesy by radio interferometry: Effects of atmospheric modelling errors on estimate of baseline length, *Radio Sci.*, *2*, 1593–1607, 1985.

De Tomasi, F., M. R. Perrone, and M. L. Protopapa, Ground-based Raman-lidar for day and night measurements of water vapor in boundary layer, *Il Nuovo Cimento*, *23C*(6), 587–596, 2000.

Dong, D.-N., and Y. Bock, Global Positioning System network analysis with phase ambiguity resolution applied to crustal deformation studies in California, *J. Geophys. Res.*, *94*(B4), 3949–3966, 1989.

Duan, J., et al., GPS meteorology: Direct estimation of the absolute value of precipitable water, *J. Appl. Meteorol.*, *35*, 830–838, 1996.

Elgered, G., J. L. Davis, T. A. Herring, and I. I. Shapiro, Geodesy by radio interferometry: Water vapor radiometry for estimation of the wet delay, *J. Geophys. Res.*, *96*(B4), 6541–6555, 1991.

Elgered, G., J. M. Johansson, and J. L. Davis, Using microwave radiometry and space geodetic systems for studies of atmospheric water-vapour variations, in *Microwave Radiometry and Remote Sensing of the Environment*, edited by D. Solimini, pp. 69–78, VSP Int. Sci, Zeist, Netherlands, 1995.

Elliott, W. P., and D. J. Gaffen, On the utility of radiosonde humidity archives for climate studies, *Bull. Am. Meteorol. Soc.*, *72*, 1507–1520, 1991.

England, M. N., R. A. Ferrare, S. H. Melfi, D. N. Whiteman, and T. A. Clark, Atmospheric water vapor measurements: Comparison of microwave radiometry and lidar, *J. Geophys. Res.*, *97*(D1), 899–916, 1992.

Feltz, W. F., W. L. Smith, R. O. Knuteson, H. R. Revercomb, H. B. Howell, and H. H. Woolf, Meteorological applications of temperature and water vapor retrievals from the ground-based atmospheric emitted radiance interferometer (AERI), *J. Appl. Meteorol.*, *37*, 857–875, 1998.

Garrison, J., and G. Adler, Estimation of precipitable water over the United States for application to the division of solar radiation into its direct and diffuse components, *Sol. Energy*, *44*, 225–241, 1990.

Ge, M., E. Calais, and J. Haase, Reducing satellite orbit error effects in near real-time GPS zenith tropospheric delay estimation for meteorology, *Geophys. Res. Lett.*, *27*(13), 1915–1918, 2000.

Georgiadou, Y., and A. Kleusberg, On carrier signal multipath effects in relative GPS positioning, *Manuscr. Geod.*, *13*(3), 172–179, 1988.

Giver, L. P., C. Chackerian, and V. Prasad, Visible and near infrared $H_2{}^{16}O$ line intensity corrections for HITRAN-96, *J. Quant. Spectrosc. Radiat. Transfer*, *66*(1), 101–105, 2000.

Guerova, G., E. Brockmann, J. Quiby, F. Schubiger, and C. Mätzler, Verification of the operational NWP model with Swiss GPS network AGNES, paper presented at Annual Meeting, GPS for Meteorology Session, Can. Geophys Union, Ottawa, Ontario, Canada, 17 May 2001.

Gueymard, C., Analysis of monthly average atmospheric precipitable water vapor and turbidity in Canada and the northern United States, *Sol. Energy*, *53*, 57–71, 1994.

Gutman, S. I., and S. G. Benjamin, The role of ground-based GPS meteorological observations in numerical weather prediction, *GPS Solut*, *4*(4), 16–24, 2001.

Hall, A., and S. Manabe, Effect of water vapor feedback on internal and anthropogenic variations of the global hydrologic cycle, *J. Geophys. Res.*, *105*(D5), 6935–6944, 2000.

Halthore, N. R., F. E. Thomas, B. N. Holben, and B. L. Markham, Sun photometric measurements of atmospheric water vapor column abundance in the 940-nm band, *J. Geophys. Res.*, *102*(D4), 4343–4352, 1997.

Held, I. M., and B. J. Soden, Water vapor feedback and global warming, *Annu. Rev. Energy Environ*, *25*, 445–475, 2000.

Héroux, P., M. Caissy, and J. Gallace, Canadian active control data acquisition and validation, *Proc. 1993 IGS (International GPS Service for Geodynamics) Workshop*, pp. 49–58, Nat. Resour. Can. Geodetic Surv. Div, Ottawa, Ontario, Canada, 1993.

Hoerling, M. P., and A. Kumar, Why do North American climate anomalies differ from one El Niño event to another?, *Geophys. Res. Lett.*, *24*(9), 1059–1062, 1997.

Hoff, R. M., Vertical structure of Arctic haze observed by Lidar, *J. Appl. Meteorol.*, *27*, 125–139, 1988.

Hogg, D. C., F. O. Guiraud, J. B. Snider, M. T. Decker, and E. R. Westwater, A steerable dual-channel microwave radiometer for measurements of water vapor and liquid in the troposphere, *J. Clim. Appl. Meteorol.*, *22*, 789–806, 1983.

Holben, B. N., et al., AERONET: A federated instrument network and data archive for aerosol characterization, *Remote Sens. Environ.*, *66*, 1–16, 1998.

Holben, B. N., et al., An emerging ground-based aerosol climatology: Aerosol optical depth from AERONET, *J. Geophys. Res.*, *106*(D11), 12,067–12,097, 2001.

Hurn, J., *Differential GPS Explained* (*Revision 4*/*96*), 55 pp., Trimble Navig., Sunnyvale, Calif.,1993.

Ingold, T., R. Peter, and N. Kämpfer, Weighted mean tropospheric temperature and transmittance determination at millimeter-wave frequencies for ground-based applications, *Radio Sci.*, *33*, 905–918, 1998.

IGS, Rep. *Annu. Rep. IGS*, 55 pp., Jet Propuls. Lab., central bureau (eds.), Pasadena, Calif., 2002.

Iwabuchi, T., I. Naito, and N. Mannoji, A comparison of global positioning system retrieved precipitable water vapor with the numerical weather prediction analysis data over the Japanese Islands, *J. Geophys. Res.*, *105*(D4), 4573–4585, 2000.

Kasischke, E. S., H. H. F. French, P. Harrell, N. L. Christensen Jr., S. L. Ustin, and D. Barry, Monitoring of wildfires in boreal forests using large area AVHRR NDVI composite image data, *Remote Sens. Environ.*, *45*(1), 61–71, 1993.

Kay, M. J., and M. Box, Radiative effects of absorbing aerosols and the impact of water vapor, *J. Geophys. Res.*, *105*(D10), 12,221–12,234, 2000.

Kouba, J., and P. Héroux, Precise point positioning using IGS orbit and clock products, *GPS Solut.*, *5*(2), 12–28, 2001.

Kouba, J., Y. Mireault, G. Beutler, T. Springer, and G. Gendt, A discussion of IGS solutions and their impact on geodetic and geophysical applications, *GPS Solut.*, *2*(2), 3–15, 1998.

Kuo, Y.-H., Y. R. Guo, and E. R. Westwater, Assimilation of precipitable water measurements into a mesoscale model, *Mon. Weather Rev.*, *121*, 1215–1238, 1993.

Kuo, Y.-H., X. Zou, and Y. R. Guo, Variational assimilation of precipitable water using a non-hydrostatic mesoscale adjoint model. part 1: Moisture retrieval and sensitivity experiments, *Mon. Weather Rev.*, *124*, 122–147, 1996.

Kunysz, W., A novel GPS survey antenna, *Rep. Novatel Inc.*, 8 pp., Novtel, Inc., Calgary, Alberta, Canada, 2000.

Lachapelle, G., W. Falkenberg, D. Neufeldt, and P. Kielland, Marine DGPS using code and carrier in a multi-path environment, *Proc. Satell. Div. Int. Tech. Meet. GPS '89*, pp. 343–347, Can. Hydrographic Assoc., Ottawa, Ontario, Canada, 1990.

Latif, M., R. Kleeman, and C. Eckert, Greenhouse warming, decadal variability, or El Niño? An attempt to understand the anomalous 1990, *Rep. 175*, Max-Planck-Institut für Meteorol., Hamburg, Germany, 1995.

Leckner, B., The spectral distribution of solar radiation at Earth's surface: Elements of a model, *Sol. Energy*, *20*, 143–150, 1978.

Liou, Y.-A., C.-Y. Huang, and Y.-T. Teng, Precipitable water observed by ground-based GPS receivers and microwave radiometry, *Earth Planets Space*, *52*, 445–450, 2000.

MacDonald, A. E., Y. Xie, and R. H. Ware, Diagnosis of three-dimensional water vapor using a GPS network, *Mon. Weather Rev.*, *130*, 386–397, 2002.

Markham, B. L., J. S. Schafer, B. N. Holben, and R. N. Haltore, Atmospheric aerosol and water vapor characteristics over north central Canada during BOREAS, *J. Geophys. Res.*, *102*(D24), 29,737–29,745, 1997.

Mätzler, C., L. Martin, G. Guerova, and T. Ingold, Assessment of integrated-water-vapor data at Bern from GPS, Sun photometry, microwave radiometry and radiosonde, paper presented at Workshop of COST Action 716, Exploitation of Ground-Based GPS Meteorology, GeoForschungsZentrum Potsdam, Potsdam, Germany, 28–29 January 2002.

Mendes, V. B., G. Prates, L. Santos, and R. B. Langley, An evaluation of models for the determination of the weighted mean temperature of the atmosphere, *Proc. Inst. of Navig. 2000 Natl. Tech. Meet.*, pp. 433–438, Univ. of New Brunswick, New Brunswick, Canada, 2000.

Muellerschoen, R. J., W. I. Bertiger, and M. F. Lough, Results of an Internet-based dual-frequency global differential GPS system, *Proc. Natl. Tech. Meet. Ion World Cong.*, pp. 220–225, NASA Jet Propuls. Lab., Washington, D.C., 2000.

Neilan, R. E., J. F. Zumberge, G. Beutler, and J. Kouba, The International GPS service: A global resource for GPS applications and research, *Proc. ION GPS'97 10th Int. Tech. Meet.*, pp. 883–889, Int. GPS Serv., Ottawa, Ontario, Canada, 1997.

Niell, A. E., Global mapping functions for the atmosphere delay at radio wavelengths, *J. Geophys. Res.*, *101*(B2), 3227–3246, 1996.

Niell, A. E., A. J. Coster, F. S. Solheim, V. B. Mendes, P. C. Toor, R. B. Langley, and C. A. Upham, Comparison of measurements of atmospheric wet delay by radiosonde water vapor radiometer, GPS and VLBI, *J. Atmos. Oceanic Technol.*, *18*, 830–850, 2001.

Ohtani, R., and I. Naito, Comparisons of GPS-derived precipitable water vapors with radiosonde observations in Japan, *J. Geophys. Res.*, *105*(D22), 26,917–26,929, 2000.

Prabhakara, C., D. A. Short, and B. E. Volmer, El Niño and atmospheric water vapor: Observations from Nimbus 7 SMMR, *J. Climatol. Appl. Meteorol.*, *24*, 1311, 1985.

Reigber, C., G. Gendt, G. Dick, and M. Tomassini, Water vapor monitoring for weather forecasts, *GPS World*, *13*(1), 18–27, 2002.

Rocken, C., R. Ware, T. V. Hove, F. Solheim, C. Alber, J. Johnson, M. Bevis, and S. Businger, Sensing atmospheric water vapor with the global positioning system, *J. Geophys. Res.*, *20*(23), 2631–2634, 1993.

Rocken, C., J. M. Johnson, J. J. Braun, H. Kawawa, Y. Hatanaka, and T. Imakiire, Improving GPS surveying with modeled ionospheric corrections, *Geophys. Res. Lett.*, *27*(23), 3821–3824, 2000.

Rothman, L. S., et al., The HITRAN molecular spectroscopic database and HAWKS (HITRAN Atmospheric Workstation): 1996 edition, *J. Quant. Spectrosc. Radiat. Transfer*, *60*(5), 665–710, 1998.

Saastamoinen, J., Atmospheric correction for troposphere and stratosphere in radio ranging of satellites, in *The Use of Artifical Satellites for Geodesy*, *Geophys. Monogr. Ser.*, vol. 15, edited by S. W. Henriksen et al., pp. 247–251, AGU, Washington, D. C., 1972.

Schmid, B., K. J. Thome, P. Demoulin, R. Peter, C. Mätzler, and J. Sekler, Comparison of modeled and empirical approaches for retrieving columnar water vapor from solar transmittance measurements in the 0.94-μm region, *J. Geophys. Res.*, *101*(D5), 9345–9358, 1996.

Schmid, B., et al., Comparison of columnar water-vapor measurements from solar transmittance methods, *Appl. Opt.*, *40*(12), 1886–1896, 2001.

Serreze, M. C., M. C. Rehder, R. G. Barry, and J. D. Kahl, A climatological data base of Arctic water vapor characteristics, *Polar Geogr. Geol.*, *18*(1), 63–75, 1994.

Sierk, B., B. Kurki, H. Becker-Ross, S. Florek, R. Neubert, L. P. Kruse, and H.-G. Kahle, Tropospheric water vapor derived from solar spectrometer, radiometer, and GPS measurements, *J. Geophys. Res.*, *102*(B10), 22,411–22,424, 1997.

Smirnov, A., B. N. Holben, T. F. Eck, O. Dubovik, and I. Slutsker, Cloud screening and quality control algorithms for the AERONET data base, *Remote. Sens. Environ.*, *73*, 337–349, 2000.

Smith, W. L., W. F. Feltz, R. O. Knuteson, H. R. Revercomb, H. B. Howell, and H. Woolf, The retrieval of planetary boundary layer structure using ground based infrared spectral radiance measurements, *J. Atmos. Oceanic Technol.*, *16*, 323–333, 1998.

Thériault, J.-M., C. Bradette, and J. Gilbert, Atmospheric remote sensing with a ground-based spectrometer system, *Proc. SPIE Annu. Symp. Aerospace/Defence Sens. Control.*, *2744*, 664–672, 1996.

Tomasi, C., S. Marani, V. Vitale, F. Wagner, A. Cacciari, and A. Lupi, Precipitable water from infrared sun-photometric measurements analysed using atmospheric hygrometry techniques, *Tellus, Ser. B.*, *52*, 734–749, 2000.

Tregoning, P., R. Boers, D. O'Brien, and M. Hendy, Accuracy of absolute precipitable water vapor estimates from GPS observations, *J. Geophys. Res.*, *103*(D22), 23,701–23,710, 1998.

Van Dierendonck, A. J., P. Fenton, and T. Ford, Theory and performance of narrow correlator spacing in a GPS receiver, *Proc. Tech. Meet.*, pp. 115–224, A-J Syst., Lautertal, Germany, 1992.

Wade, C. G., An evaluation of problems affecting the measurement of low relative humidity on the U.S. radiosonde, *J. Atmos. Oceanic Technol*, *11*, 687–700, 1994.

Wade, C. G., Calibration and data reduction problems affecting the national weather service radiosonde humidity measurements, paper presented at Am. Meteorol. Soc. 9th Symp. on Meteorol. Obs. and Instrum., Charlotte, N. C., 27–31 March 1995.

Ware, R., D. Fulker, S. Stein, D. Anderson, S. Avery, R. Clark, K. Droegemeier, J. Kuettner, J. Minster, and S. Sorooshian, SuomiNet: A real-time national GPS network for atmospheric research and education, *Bull. Am. Meteorol. Soc.*, *81*, 677–694, 2000.

Webster, P. J., and T. N. Palmer, The past and future of El Niño, *Nature*, *390*, 562–564, 1997.

Westwater, E. R., The accuracy of water vapor and cloud liquid water determination by dual-frequency ground-based microwave radiometry, *Radio Sci.*, *13*, 677–685, 1978.

Westwater, E. R., J. B. Snider, and M. J. Falls, Ground-based radiometric observations of atmospheric emission and attenuation at 20.6, 31.65, and 90.0 GHz: A comparison of measurements and theory, *IEEE Trans. Antennas Propag.*, *38*, 1569–1580, 1990.

Wolfe, D. E., and S. I. Gutman, Developing an operational, surface-based, GPS, water vapor observing system for NOAA: Network design and results, *J. Atmos. Oceanic Technol.*, *17*, 426–439, 2000.

Yang, X., B. H. Sass, G. Elgered, J. M. Johansson, and T. R. Emardson, A comparison of precipitable water vapor by a NWP simulation and GPS observations, *J. Appl. Meteorol.*, *38*, 941–956, 1999.

Zumberge, J. F., M. B. Heflin, D. C. Jefferson, M. M. Watkins, and F. H. Webb, Precise point positioning for the efficient and robust analysis of GPS data from large networks, *J. Geophys. Res*, *102*(B3), 5005–5017, 1997.

A. I. Bokoye, Laboratoire Interdisciplinaire en Sciences de l'Environnement/Ecosystèmes Littoraux et Côtiers, UMR CNRS 8013 Université du Littoral Côte d'Opale: Maison de la Recherche en Environnement Naturel, 32 Av. Foch, Wimereux F-62930, France. (bokoye@mren2.univ-littoral.fr)

P. Cliche, N. T. O'Neill, and A. Royer, Centre d'Applications et de Recherches en Telédétection, Université de Sherbrooke, Sherbrooke, Quebec, Canada J1K 2R1. (noneill@courrier.usherb.ca; aroyer@courrier.usherb.ca)

G. Fedosejevs and P. M. Teillet, Canada Centre for Remote Sensing, Ottawa, Ontario, Canada K1A 0Y7.

L. J. B. McArthur, Meteorological Service of Canada, Downsview, Ontario, Canada M3H 5T4. (bruce.mcarthur@ec.gc.ca)

J.-M. Thériault, Defence Research and Development Canada, Valcartier, 2459 boulevard Pie-XI nord, Val Bélair, Quebec, Canada G3J 1X5.